

Low half-wave voltage and high electro-optic effect in hybrid polymer/sol-gel waveguide modulators

Y. Enami,^{a)} C. T. DeRose, C. Loychik, D. Mathine, and R. A. Norwood
College of Optical Sciences, University of Arizona, Tucson, Arizona 85721

J. Luo and A. K.-Y. Jen

Department of Material Science and Engineering, University of Washington, Seattle, Washington 98195-2120

N. Peyghambarian

College of Optical Sciences, University of Arizona, Tucson, Arizona 85721

(Received 3 July 2006; accepted 25 July 2006; published online 3 October 2006)

The authors report on hybrid electro-optic (EO) polymer-sol-gel modulators with low half-wave voltage (V_π) and low insertion loss. Larger EO coefficient r_{33} results from the high poling field achieved when EO polymer is sandwiched between sol-gel cladding layers. The reduced interelectrode distance (d) resulting from the elimination of the sol-gel core layer in the active region further reduces V_π . Straight channel phase modulators operate with $V_\pi=4.2$ V at 1550 nm using a reduced d of 11.5 μm , which corresponds to an r_{33} of 78 pm/V, among the highest r_{33} reported. The authors also examine a Mach-Zehnder modulator with $V_\pi=3.9$ V using a conventional d of 15 μm . © 2006 American Institute of Physics. [DOI: 10.1063/1.2354440]

Electro-optic (EO) polymers with large EO coefficients and good long-term stability have been studied for photonic device applications such as ultrahigh-speed optical communication, terahertz generation, RF links, ultrafast spatial light modulators, and millimeter wave sensors. In particular, polymeric EO modulators have attracted attention because of their suitability for high-speed modulation and low voltage operation, due to the low dielectric dispersion and large EO coefficients of EO polymers. Ultrahigh speeds¹ up to 110 GHz and low half-wave voltages (V_π) and interaction length products² of 4.2 V cm have been demonstrated for polymeric EO modulators using an all polymer approach. All polymeric waveguide EO modulators generally consist of an EO polymer core and passive polymer cladding, and have shown relatively large coupling losses³ to standard single mode fiber because of the thin EO polymer core layer that is required to maintain single mode operation. This results from the large refractive index difference between the EO polymer core and the passive polymer cladding. Furthermore, unstable coupling can exist between single mode fibers and all-EO polymer waveguides because of the altered mode field diameter in the polymeric waveguides caused by the time dependent refractive indices of the EO polymers.³ Hybrid waveguides offer potential improvement not only for fiber coupling loss and stability but also for efficient poling of EO polymers when a low resistance cladding layer such as organically modified sol-gel glass is employed. Recent reports have shown relatively low EO coefficients (25 pm/V) in all polymeric modulators⁴ because of the use of high resistivity polymer cladding layers, even though the EO polymer itself has shown a single layer EO coefficient of 88 pm/V, obtained when the EO polymer film was poled between electrodes without the presence of cladding layers.

In contrast to propagation loss, coupling loss and device stability can be improved by using hybrid waveguides. Re-

cently, hybrid EO polymer/sol-gel glass waveguide modulators were reported⁵⁻⁸ to reduce optical coupling loss down to 1 dB per end face^{5,7} when using standard communication fiber, to improve waveguiding and EO modulation stability, and to reduce fabrication cost by using an all-wet-etching process. Light coupled from a single mode fiber to the sol-gel input waveguide was adiabatically transferred to an EO polymer waveguide and then back to a sol-gel output waveguide through low-loss vertical tapers [with a low taper angle of 0.9°–3.6°] defined in the sol-gel overcladding. After this first demonstration,⁵ a laterally confined structure was demonstrated in a sol-gel overcladding channel that increased mode confinement in the EO polymer by virtue of eliminating lateral radiation. This enabled a 0.9 μm thick EO polymer overlayer to be used and resulted in reducing the V_π by a factor of 4 due to the larger mode overlap integral.⁷ Phase modulators using straight channel hybrid waveguides demonstrated V_π of 13 and 22 V for 2.4 and 1.4 cm long electrodes,^{7,8} respectively, at 1550 nm. A Mach-Zehnder (MZ) modulator was also demonstrated with a V_π of 20 V for a 1.4 cm electrode using contact poling for a single hybrid waveguide arm with an insertion loss of 8 dB at 1550 nm.⁸ For these demonstrations, the EO polymer consisted of the chromophore⁶ dibutylaminobenzene-thiophene stilbene tricyanovinyl doped into the polyquinoline matrix PQ-100, with r_{33} values ranging from 25 to 30 pm/V achieved in the modulators and an optical loss of 2.2 dB/cm at 1550 nm.⁷ Here, we report on a hybrid waveguide structure with reduced V_π achieved by adopting a reduced interelectrode spacing in the active region and by attaining a higher r_{33} coefficient. The higher r_{33} results from the increased poling field afforded by the EO polymer sandwiched between sol-gel layers, suppression of dielectric breakdown, and improvements in the EO polymer itself.

A schematic of a hybrid EO polymer/sol-gel waveguide is shown in Fig. 1. The hybrid waveguide has two passive regions and an active region with an EO polymer layer. The sol-gel channel waveguide consists of a rectangular core sur-

^{a)}Electronic mail: enami@email.arizona.edu

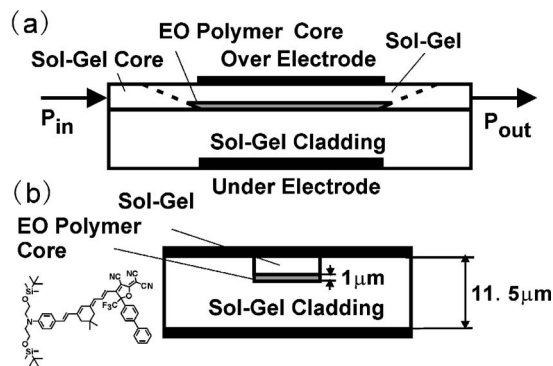


FIG. 1. Schematic of the hybrid EO polymer/sol-gel waveguide modulator: (a) side view and (b) cross section in the active region.

rounded by sol-gel cladding. The EO polymer core layer is vertically and laterally confined in the sol-gel cladding as shown in Fig. 1(b), in order to confine the mode in the EO polymer layer. In both ends of the central active region of the hybrid waveguide, the sol-gel core is vertically tapered to have an adiabatic transition between the EO polymer core and the sol-gel core. In the active region [see Fig. 1(a)], the total interelectrode spacing is 11.5 μm and the EO polymer layer thickness is 1 μm. The sol-gel layers sandwiching the EO polymer layer allow for the application of high poling fields (>100 V/μm) to the EO polymer layer because the sol-gel layer has much lower resistivity than the EO polymer at the poling temperature of 150 °C. Sol-gel layers also prevent dielectric breakdown in the EO polymer layer due to reduction of the poling current in the relatively thinner regions of the EO polymer layer, which can become a trigger for avalanche dielectric breakdown during the application of high poling fields (e.g., >100 V/μm).⁹ The overcladding layer deposited on the sol-gel core together with the laterally tapered core size in the passive regions and smaller refractive index difference (e.g., 0.4%) in the passive regions provides optimized coupling⁶ between single mode fiber (SMF-28TM) and the hybrid waveguide, even though the sol-gel core is exposed to air in the passive regions in this work to simplify the processing. The sol-gel side cladding has a selectively exposed window with the same width as the sol-gel core; the EO polymer is filled into this window. Vertical tapers in the sol-gel core reduce the thickness of the EO polymer gradually when less than 10 wt % EO polymer in solution is spin coated onto the sol-gel structure. From previous work, we determined a target taper length of 500 μm for the 3.5 μm thick core in order to obtain a few degree taper angle in the sol-gel core. On the EO polymer, the sol-gel layer is coated to ensure an adiabatic transition between the sol-gel core and the EO polymer core; the upper cladding layer also functions as a buffer layer to prevent optical loss due to optical absorption from the top electrode.

The mode intensity profile was calculated for this hybrid structure and the mode overlap integral is estimated to be 80%, based on a three-dimensional beam propagation method and finite-difference method approach. In these calculations, the refractive indices for the sol-gel core, sol-gel cladding, and EO polymer are taken to be 1.500, 1.487, and 1.632, respectively. The thicknesses of the sol-gel core and the undercladding are 3.5 and 7 μm, respectively, and the thickness of the EO polymer is 1 μm, which can be further

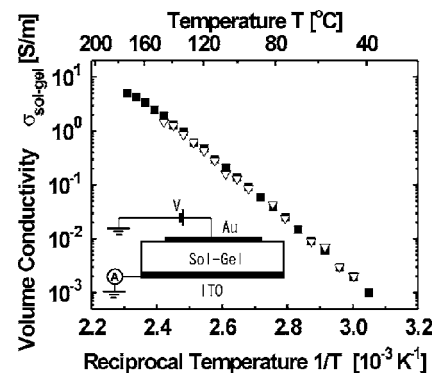


FIG. 2. Reciprocal temperature dependence of the volume conductivity for a 12 μm thick sol-gel film when 400 V (closed squares) and 600 V (open down triangles) are applied between the ITO and gold electrodes. The inset shows the experimental setup for the measurement.

reduced in order to increase the modulating field without significant impact on the overlap integral.

Two component formulation solutions were prepared based on the organically modified sol-gel precursor [methacryloyloxy propyltrimethoxysilane (MAPTMS)] and an index modifier [zirconium(IV)-*n*-propoxide] with molar ratios of 95(MAPTMS)/5 mol % and 85(MAPTMS)/15 mol % for the cladding and core, respectively; 0.1N HCl was used to accelerate hydrolysis. A photoinitiator, IRGACURE 184 (Ciba), was added to the core solutions to allow for photolithographic definition of the core and side cladding, which were irradiated by UV (275 W, $\lambda_{\text{peak}}=360$ nm) through photomasks in a mask aligner and developed in isopropanol for 15–20 s. Sol-gel solutions were spin coated at 2800 rpm for the core and side cladding, and at 3500 rpm for the undercladding. Core and side cladding layers were soft baked at 90 °C for 10 min prior to wet etching. A 7 μm thick undercladding was coated on a Si(100) substrate with a 100 nm Ti under electrode. Thinner undercladding layers reduce the interelectrode distance, thereby further lowering V_{π} . After the undercladding layer was baked at 150 °C for 1 h, the side cladding for the core with widths ranging from 2 to 10 μm was spin coated, photolithographically exposed, and wet etched, resulting in a laterally confined structure in the cladding. The core layer was spin coated to fill in the trench formed by the sidewall of the side cladding, and wet etched after UV radiation through a gray-scale mask, to give vertical tapers in the two separated sol-gel cores from the passive regions into the active region.

The EO polymer solution was spin coated to give a 1 μm thick EO polymer core. The EO polymer is a guest-host system, which has 25 wt % AJLS102 chromophore (see Fig. 1) in an amorphous polycarbonate matrix, with a refractive index of 1.632 at 1550 nm and a glass transition temperature of 150 °C. After the EO polymer was baked at 85 °C for 12 h to remove the solvent, a top sol-gel layer was spin coated to confine the EO polymer vertically between the sol-gel layers, and hard baked at 150 °C for 1 h.

To enable efficient poling of the EO polymer between the sol-gel layers, the volume conductivity of the sol-gel layer was examined in the temperature range from 40 to 180 °C with the experimental setup as shown in the inset of Fig. 2. Voltages of 400 and 600 V were applied to a 12 μm thick sol-gel layer sandwiched between indium tin oxide (ITO) and a gold electrode. The temperature depen-

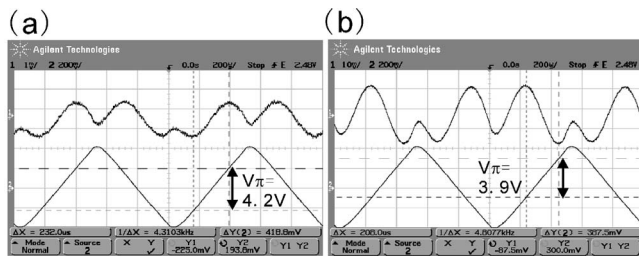


FIG. 3. Low frequency transfer function measurement at 1550 nm. Oscilloscope shows the traces of modulated voltage and optical signal. Upper: optical output signal. Lower: applied voltage. (a) Phase modulator with interelectrode distance of 11.5 μm shows $V_{\pi}=4.2$ V. (b) Push-pull poled Mach-Zehnder modulator with interelectrode distance of 15 μm shows $V_{\pi}=3.9$ V.

dence of the volume conductivity was rendered as an Arrhenius plot as shown in Fig. 2. Sol-gel layers also have much larger conductivity than soda-lime glass.¹⁰ The volume conductivity of the MAPTMS sol-gel was 1–4 S/m for applied voltages of 400 and 600 V in the poling temperature range of 150–185 $^{\circ}\text{C}$, which was larger than the volume conductivity of the EO polymer (10^{-8} – 10^{-6} S/m) by seven to nine orders of magnitude, when a poling field of 50–95 V/ μm was applied for the same temperature range in a separate apparatus.

From these experiments, we deduced that substantially all of the poling voltage would be delivered to the EO polymer layer in the multilayer structure of an EO polymer/sol-gel hybrid modulator. Related studies have indicated that neither the sol-gel layer nor the EO polymer exhibits Ohmic behavior over the full electric field and temperature range considered.¹¹ The EO polymer was contact poled with an applied voltage of 1 kV with poling current of 190 μA at 150 $^{\circ}\text{C}$. This relatively high poling current density for the hybrid modulator indicated that the EO polymer was efficiently poled in the multilayer, in contrast to recent reports^{4,12} in which the EO coefficient of the EO polymer in all polymeric modulators was determined to be $\sim 30\%$ of that of singly poled EO polymer layer because of the low conductivity of the cladding materials.⁴

V_{π} was examined for a phase modulator with a 2.4 cm electrode after phase modulation was converted to intensity modulation using a cross-polarization setup.⁶ Linearly polarized light (0.4 mW at 1550 nm wavelength) at $+45^{\circ}$ was coupled from a single mode fiber SMF-28TM into the hybrid waveguide through a polarization controller. Exiting light was focused through an analyzer (polarized at -45° or $+45^{\circ}$) onto a detector by a 20 \times microscope objective lens. The time variations of the applied voltage at 1 kHz and of the detected optical power were observed simultaneously on an oscilloscope as illustrated in Fig. 3(a). V_{π} was determined to be 4.2 V in the phase modulator with 2.4 cm electrodes, which corresponds to an r_{33} of 78 pm/V at 1550 nm. The EO coefficient for the EO polymer poled in the hybrid modulator was usually larger than that for a single layer EO film poled between ITO glass and gold electrodes when the EO polymer was contact poled (100 V/ μm at 150 $^{\circ}\text{C}$); this represents a significant breakthrough, compared to previous re-

ports for EO modulators using the latest EO polymers.^{4,12} The optical insertion loss was 15 dB at 1550 nm for 3 cm hybrid modulator, which can be reduced by using an overlcladding on the sol-gel core with a longitudinally aligned vertically tapered cladding structure in the active region and a laterally tapered core in the passive region to provide a larger mode field diameter suitable for coupling with SMF-28TM. A Mach-Zehnder modulator was also examined using the previous hybrid approach with push-pull poling for the two arms. V_{π} was 3.9 V at 1550 nm for a 2.4 cm electrode device with an interelectrode distance of 15 μm as shown in Fig. 3(b); push-pull poling voltages of +400 and –400 V were applied at 150 $^{\circ}\text{C}$. With further reduction of the sol-gel undercladding thickness the Mach-Zehnder modulator with push-pull poling in this reported approach would result in subvolt V_{π} 's with relatively low insertion loss (5–10 dB).

In summary, we successfully fabricated hybrid electro-optic polymer/sol-gel waveguide modulators to realize higher EO coefficients, which lead to lower V_{π} less than 4 V when a poling voltage of 1 kV was used for contact poling in the hybrid modulator. The demonstrated EO coefficient showed values equal to or above those of singly poled EO polymer layers because of the much higher volume conductivity at this poling temperature for the sol-gel in comparison to that of the EO polymer. At the same time, the sol-gel cladding provides low-cost photopatternability, good optical properties, and excellent dielectric properties in the operating temperature range.

The authors would like to acknowledge support from the National Science Foundation MDITR Science and Technology Center and Nitto Denko Technical in Oceanside, CA.

¹D. Chen, H. R. Fetterman, A. Chen, W. H. Steier, L. R. Dalton, W. Wang, and Y. Shi, Appl. Phys. Lett. **70**, 3335 (1997).

²H. Zhang, M.-C. Oh, A. Szep, W. H. Steier, C. Zhang, L. R. Dalton, H. Erlig, Y. Chang, D. H. Chang, and H. R. Fetterman, Appl. Phys. Lett. **78**, 3136 (2001).

³M.-C. Oh, H. Zhang, C. Zhang, H. Erlig, Y. Chang, B. Tsap, D. Chang, A. Szep, W. H. Steier, H. R. Fetterman, and L. R. Dalton, IEEE J. Sel. Top. Quantum Electron. **7**, 826 (2001).

⁴Y.-H. Kuo, J. Luo, W. H. Steier, and A. K.-Y. Jen, IEEE Photonics Technol. Lett. **18**, 175 (2006).

⁵Y. Enami, G. Meredith, N. Peyghambarian, M. Kawazu, and A. K.-Y. Jen, Appl. Phys. Lett. **82**, 490 (2003).

⁶Y. Enami, M. Kawazu, A. K.-Y. Jen, G. Meredith, and N. Peyghambarian, J. Lightwave Technol. **21**, 2053 (2003).

⁷Y. Enami, G. Meredith, N. Peyghambarian, and A. K.-Y. Jen, Appl. Phys. Lett. **83**, 4692 (2003).

⁸Y. Enami, A. K.-Y. Jen, G. Meredith, and N. Peyghambarian, Proc. SPIE **5351**, 28 (2004).

⁹M. Sprave, R. Blum, and M. Eich, Appl. Phys. Lett. **69**, 2962 (1996).

¹⁰Y. Enami, P. Poyhonen, D. L. Mathine, A. Bashar, P. Madasamy, S. Honkanen, B. Kippelen, N. Peyghambarian, S. R. Marder, A. K.-Y. Jen, and J. Wu, Appl. Phys. Lett. **76**, 1086 (2000).

¹¹C. T. DeRose, Y. Enami, C. Loychik, R. A. Norwood, D. Mathine, M. Fallahi, N. Peyghambarian, J. Luo, A. Jen, M. Kathaperumal, and M. Yamamoto, Appl. Phys. Lett. (to be published).

¹²S.-K. Kim, Y.-C. Hung, B.-J. Seo, K. Geary, W. Yuan, B. Bortnik, H. R. Fetterman, C. Wang, W. H. Steier, and C. Zhang, Appl. Phys. Lett. **87**, 061112 (2005).